

RSC Advances



This is an *Accepted Manuscript*, which has been through the Royal Society of Chemistry peer review process and has been accepted for publication.

Accepted Manuscripts are published online shortly after acceptance, before technical editing, formatting and proof reading. Using this free service, authors can make their results available to the community, in citable form, before we publish the edited article. This *Accepted Manuscript* will be replaced by the edited, formatted and paginated article as soon as this is available.

You can find more information about *Accepted Manuscripts* in the [Information for Authors](#).

Please note that technical editing may introduce minor changes to the text and/or graphics, which may alter content. The journal's standard [Terms & Conditions](#) and the [Ethical guidelines](#) still apply. In no event shall the Royal Society of Chemistry be held responsible for any errors or omissions in this *Accepted Manuscript* or any consequences arising from the use of any information it contains.

Simultaneous determination of omethoate and dichlorvos pesticides in grain samples using palladium and graphene composite modified glassy carbon electrode

Cite this: DOI:10.1039/x0xx00000x

Received xxxxxxxxxxxxxxxx
Accepted xxxxxxxxxxxxxxxx

DOI: 10.1039/x0xx00000x

www.rsc.org/

M. Siva Prasad, K. Krishnaveni, M. Dhananjayulu, V. Sreenivasulu and N.Y. Sreedhar*

An electrochemical sensor based on palladium (Pd) and graphene (Gr) composite modified glassy carbon electrode (GCE) was fabricated, characterised and used for simultaneous determination of omethoate (OMT) and dichlorvos (DCV) in grain samples. The Pd/Gr/GCE was characterized by scanning electron microscopy (SEM) and cyclic voltammetry (CV). The modified electrode displayed greatly improved voltammetric response to OMT and DCV. Square wave voltammetry (SWV) was used for individual and simultaneous determination of OMT and DCV. The conditions were optimized such as pH of buffer, applied sample volume, accumulation potential, accumulation time, square wave frequency and step potential. The well defined reduction (OMT at C=O, DCV at C=C) peaks were obtained over the potential maximum at -0.50V and -0.80V in acidic medium in phosphate buffer solution for both OMT and DCV. The low current peaks were obtained over the concentration at 3.50×10^{-8} M with detection limits 2.47×10^{-10} M and 3.28×10^{-10} M for OMT and DCV respectively. The composite modified electrode showed good stability and reproducibility. Hence, the proposed method was successfully applied for the analysis with a great assure as an economical and simple sensor with furthermore a shorter analysis time.

1. Introduction

Nanostructured materials have received emergent welfares due to their unique chemical and physical properties, depending upon their size and shape.¹ Graphene (Gr), a two dimensional carbon nanomaterial with outstanding physical and chemical properties, has become one of the most exciting topics of both fundamental science and applied research recently.² As a counterpart of graphite with well separated 2D aromatic sheets, Gr possesses the high quality of the sp^2 conjugated bond in the carbon lattice and has remarkably high electron mobility under ambient conditions with reported values.³ Moreover, Gr has a very large specific surface area with low manufacturing cost and excellent mechanical strength.⁴

Even though palladium (Pd) itself has been proven to be a suitable catalyst for electrooxidation of alcohols in alkaline media, more efforts are needed for further improvement of electrocatalytic performance of Pd-based catalysts. Supporting on materials with large surface areas such as carbon black, activated carbon, carbon nanofibers and carbon nanotube is one approach.⁵⁻⁷ Palladium nanostructures are of great interest due to their invaluable excellent catalytic performance with the properties of lower cost, high efficiency and selectivity.⁸⁻¹² A large number of carbon-carbon bond forming reactions in organic chemistry such as, Suzuki, Heck, Stille coupling, hydrogenation/dehydrogenation reactions, low temperature reduction of automobile pollutants and petroleum cracking all depend on the catalysts based upon Pd and its compounds.¹³⁻¹⁶ It was found that the combination of Pd nanostructures and carbon materials could enhance the stability and activity of the catalysts, such as carbon nanotubes, nanorods and the new emerging graphene.^{17,18} Muniyandi Rajkumar et al. reported the preparation of

single step electrochemical fabrication of highly loaded palladium nanoparticles decorated chemically reduced graphene oxide and its electrocatalytic applications.¹⁹ Qiyu Wang et al. reported synthesis of flower-shape palladium nanostructures on graphene oxide for electrocatalytic applications.²⁰ A number of scientists reported previously for the preparation of palladium and graphene composite modifies glassy carbon electrode in electrochemical applications.²¹⁻²⁵

The detection of organophosphorous compounds are of great practical importance and have received escalating interest. Omethoate (OMT) and dichlorvos (DCV) are one of the extensively used organophosphorous pesticides in India. It efficiently kills the insects in agriculture field crops. A large number of papers have been published for determination of omethoate by mass spectrometry- gas chromatography and voltammetry.²⁶⁻³⁵ Djennine et al. reported electroanalytical method for determination of dichlorvos using gold-disk microelectrodes.³⁶ Yanhong bai et al. reported reduction of dichlorvos and omethoate residues by O_2 plasma treatment.³⁷ Yugui tao et al. reported simultaneous determination of omethoate and dichlorvos by capillary electrophoresis.³⁸ Nevertheless, to the best of our knowledge, there is no electroanalytical report concerning the simultaneous determination of OMT and DCV using palladium and graphene nanocomposite modified glassy carbon electrode.

Due to the advantages of Gr and Pd nanoparticles and their synergistic effects, the Pd/Gr nanocomposite modified electrode was prepared and exhibited better electrochemical performances. The developed voltammetric sensor was successfully applied for the simultaneous determination of OMT and DCV with good electrocatalytic activity, high sensitivity, good repeatability, long term stability and low cost.

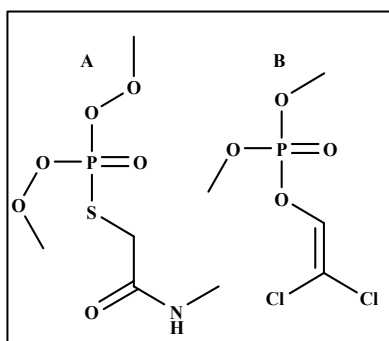


Fig.1 Molecular structure of OMT (A) and DCV (B)

2. EXPERIMENTAL

2.1. Apparatus

Electrochemical studies were carried out by Autolab PG STAT101 supplied by Metrohm Autolab B.V. Netherlands. A three electrode system comprising of a glassy carbon electrode modified with palladium (Pd) and graphene (Gr) composites served as a working electrode. Saturated Ag/AgCl/KCl as a reference electrode and Pt wire as a counter electrode. Electrode surface morphology study was carried out by Scanning electron microscopy (SEM) instrument model OXFORD INCA PENTA FETX3 CARL ZEISS from Japan. An Elico LI-120 pH meter supplied by Elico Ltd, Hyderabad, India was used to determine the pH of the buffer solution.

2.2. Chemicals and reagents

OMT and DCV were purchased from Siddarth.Inc. Hyderabad, India and their stock solutions were prepared in methanol. Phosphate buffer solution (PB) of different pH values were prepared by mixing standard solutions of 0.1M NaH_2PO_4 and 0.1M Na_2HPO_4 and adjusting the pH with 0.1M H_3PO_4 or 0.1M NaOH. All solutions were filtered through a 0.45 μm membrane filter and then degassed by sonication and evacuation. All chemicals were of analytical reagent grade and all the aqueous solutions were prepared with redistilled deionised water. These solutions were stored in the dark at 4°C.

2.3. Sample preparation of OMT and DCV in grain samples

Known amounts of the standard solutions of OMT and DCV were added to a 25 mL aliquot of grain samples (green peas and field bean from Tirupati, India) giving a final concentration of 10 μL of OMT and DCV. This sample was mixed with 10.0 mL of 0.20 mol/L PB solution (pH 5.0). No further sample treatment was done. The OMT and DCV contents were determined by three successive additions of aliquots of the standard OMT and DCV solutions.

2.4. Fabrication of Pd/Gr/GCE

Prior to the electrodeposition process, the bare glassy carbon electrode was initially polished with 0.05 μM alumina powder using BAS polishing kit and ultrasonically cleaned in water for a minute. The electrode was then washed with double distilled water and utilized for further electrodeposition. Pd/Gr nanocomposite was fabricated on the GCE surface by a simple two-step process. According to my previous paper we prepared Gr solution was drop casted on the pre-cleaned GCE and dried in an air

oven at 30°C.³⁹ Then the Gr modified GCE was shifted to an electrochemical cell with 10 mL of 0.5 M H_2SO_4 containing 1 mM H_2PdCl_4 . Consecutive cyclic voltammograms were recorded in the potential range between 1.0V to -1.0V vs Ag/AgCl/KCl reference electrode at the scan rate of 100mV/s in 100 sec. deposition time, to obtain stable voltammograms. But well defined redox voltammograms were obtained at potential -0.25V and 0.25V in 0.5M H_2SO_4 solution. The resulting modified electrode is denoted as Pd/Gr nanocomposite film modified GCE was then rinsed with double distilled water and used for further electrochemical studies. The electrode modification process and consecutive cyclic voltammograms are shown in Fig.2A &2B.

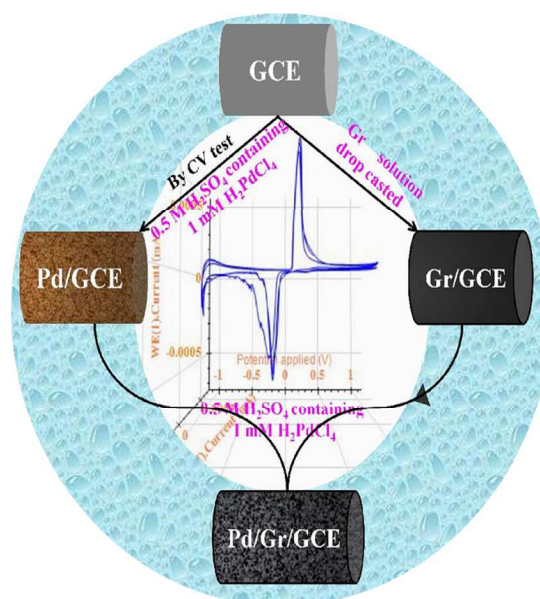


Fig. 2A Schematic graphical representation of fabrication of palladium and graphene nanocomposite on the surface of the glassy carbon electrode.

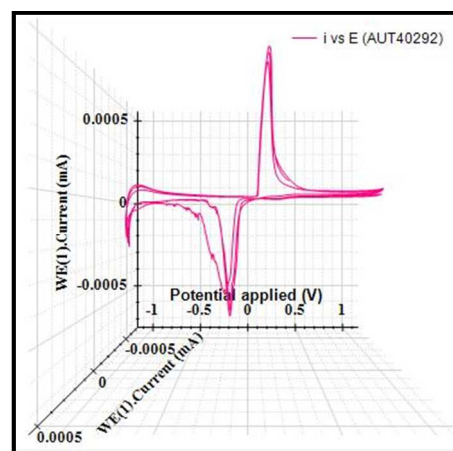


Fig. 2B Electrodeposition of Pd nanoparticles on Gr/GCE from 0.5 M H_2SO_4 containing 1.0mM H_2PdCl_4 , potential scan between -1.0V to 1.0V for three consecutive cyclic voltammograms at the scan rate of 100 mV/s.

3. RESULTS AND DISCUSSIONS

3.1. Characterisation of Pd/Gr/GCE

The cyclic voltammograms (CV) shows the electrode deposition process of Pd nanoparticles on Gr/GCE surface, which begins at the positive potential of 1.0 V and ends at the negative potential of -1.0V, shown in Fig. 3. Now, the oxidation peak of Pd particles occur at the potential of 0.25V and the reduction process takes place at the -0.25V. The fabricated Pd particles are oxidized and to form a Pd oxide layer at 0.25V on the electrode surface. After that the existing Pd oxides are reduced on the negative scans, because of hydrogen adsorption process. Throughout this repetitive cycling process, the reduction and oxidation peaks of the Pd particles were clearly growing on the Gr/GCE surface. It is obvious to the modification of Pd nanoparticles on the surface of Gr/GCE. Pd/Gr was made with different volumes of H_2PdCl_4 from 1 mg to 5 mg and the voltammetric response towards the stability, at each volume was tested by use of CV in 0.5M H_2SO_4 solution at potential of 1.0V to -1.0V in 100 sec. (Fig.3). The outcome revealed that the amount of H_2PdCl_4 increased from 2.5 mg to 4.5 mg, the redox peak current enhance linearly and the formed Pd nanoparticles outfit tightly on the surface of Gr/GCE. Once raise the amount of H_2PdCl_4 after 5 mg the current response is drop off, so the surface of Gr/GCE becomes unstable caused by Pd nanoparticles are not fabricated and it is over loaded on Gr/GCE, it's clearly shown in Fig.3 from cycle 'c' to cycle 'a'. Therefore 2.5 mg to 4.5 mg of H_2PdCl_4 is preferred as the finest amount for fabricate Pd nanoparticles on the surface of Gr/GCE by cyclic voltammetry for electroanalytical application.

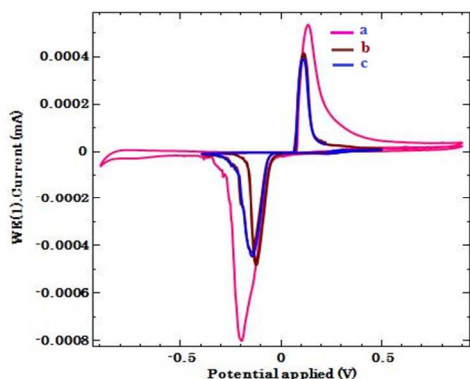


Fig. 3 Cyclic voltammetric behaviour of Pd nanoparticles on Gr/GCE, different Pd wt%, 15 wt% (a), 25 wt% (b) and 35 wt% (c) in 0.5M H_2SO_4 solution at scan rate 100 mV/s.

3.2. Morphological study

The morphology and size of the Pd nanoparticles and Pd/Gr/GCE were examined by SEM analysis. Fig. 4A depicts the formation of Pd nanoparticles over the GCE surface. Here, we can clearly see that the formed Pd nanoparticles were equally scattered on the surface of the GCE. Fig. 4B shows the SEM images of Pd/Gr/GCE which it clearly reflects that the Pd nanoparticles are homogeneously binding up throughout the Gr/GCE and the distribution of the nanoparticles are almost uniform throughout the electrode surface. The immobilized Pd/Gr nanocomposite on the surface of the GCE remains stable and there is no deformation in shape. Finally from these results, it is evident that the size and morphology for the formation of Pd nanoparticles were uniformly attached on the Gr/GCE surface.

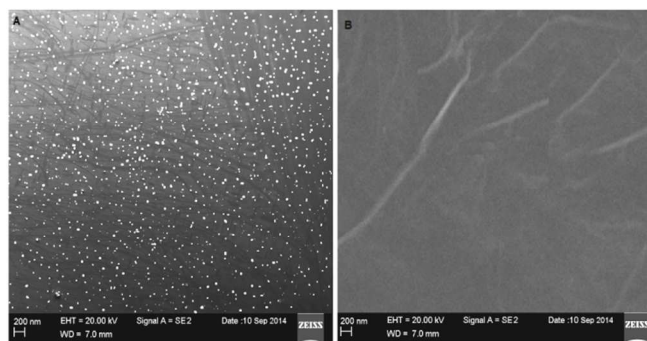


Fig. 4 SEM images of (A) Pd nanoparticles on GCE surface and (B), Pd/Gr/GCE

3.3. Simultaneous determination of OMT and DCV

Pd/Gr nanocomposite modified GCE could be directly employed for the simultaneous determination of OMT and DCV. In Fig. 5, square wave voltammetry curve 'a' represents the GCE response, curve 'b' for Pd/GCE nanocomposite film response, curve 'c' represents the Gr/GCE response and curve 'd' for the Pd/Gr/GCE response of simultaneous determination of OMT and DCV. Here we also comparing for the individual electrocatalytic reduction behaviour of the OMT and DCV at Pd/Gr/GCE. Comparing the Pd/Gr nanocomposite film with Pd nanoparticles, the Pd/Gr nanocomposite shows well define obvious electrocatalytic peaks for the determination of OMT and DCV. At the same time, only Pd nanoparticle modified electrode give two separate peaks which were not obvious like response found using Pd/Gr nanocomposite film. In this, OMT reduction takes place at around -0.45V and DCV around at -0.77V. Comparing these results, we can decide that the Pd/Gr nanocomposite film modification is more suitable for the simultaneous detection of OMT and DCV with the remaining electrodes. This may be due to the presence of Pd nanoparticles which acts as electroactive centres for the determination of these compounds. In addition, the presence of Gr as another layer enhances the peak current and potential shift supports the simultaneous determination of OMT and DCV. Subsequently, based on this framework, we conclude that the combination of Pd/Gr nanocomposite film is more suitable for these type of analysis.^{19,21}

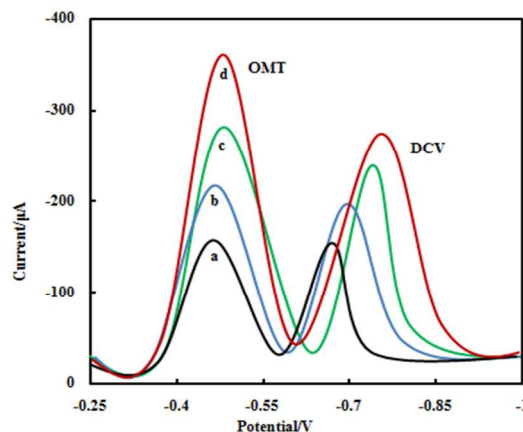


Fig. 5 SWV obtained under the optimised parameters in 0.2 mol L^{-1} PB solution (pH 5.0) for OMT and DCV at (a) GCE, (b) Pd/GCE, (c) Gr/GCE and (d) Pd/Gr/GCE, at 3.5×10^{-8} M.

3.4. Effect of accumulation potential and time

The influence of the accumulation potential on the SWV signal was deliberate with accumulation time 60 sec at Pd/Gr/GCE for 3.5×10^{-8} M of OMT and DCV. It was observed that ip value for -0.45V at pH 5.0 because of an increased accumulation rate due to the more positive alignment of molecules by the electric field at the electrode solution interface. Because of the surface adsorption of pesticide, the time effect of surface accumulation was investigated at potentials from -0.2V to -1.00V. It was found that the peak current of pesticide was not very much depended on the initial potential setting. But, it better quickly with extending time of the accumulation in the first 60 sec and then became constant afterward. The optimized accumulation time was selected as 60sec.

3.5. Effect of pH

The effect of solution pH on the response of OMT and DCV on Pd/Gr modified GCE was investigated at 3.5×10^{-8} M as shown in Fig. 6. The cathodic peak currents of OMT and DCV increased slowly with increases pH from 2.0 to 5.0 (Fig. 6). At a pH higher than 5.0, the peak currents decreased quickly with increases pH from 5.0 to 10. Hence, the peak current becomes larger with the pH increasing from 3.0 to 5.0. However, at pH over 5.0, OMT and DCV may be become protonated as citations and they start to be reduced. Also, In DCV carbonyl containing functional groups at the Pd/Gr modified electrode may become protonated and possess negative charges at pH 5.0. Therefore, electrostatic repulsion between the analytes and the electrode might be one of the reasons in the decrease of the peak currents of OMT and DCV with the pH increasing from 5.0 to 10.0. The suggested electrode reduction process is a two proton and two electron transfers.⁴⁰ In order to achieve high sensitivity, so pH 5.0 was chosen for the simultaneous detection of OMT and DCV.

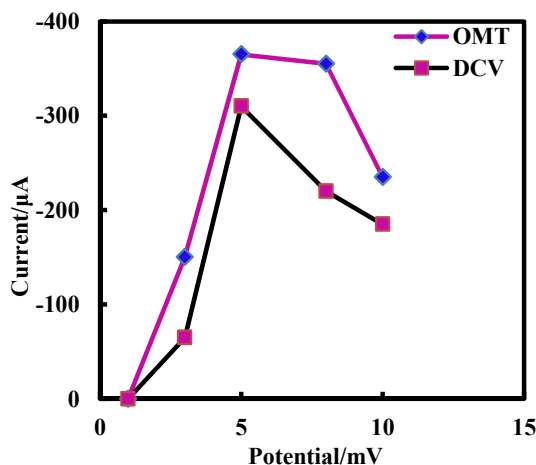


Fig.6. Effect of the pH on the peak current of OMT and DCV at Pd/Gr/GCE in PB solution at 3.5×10^{-8} M

3.6. Analytical response of OMT and DCV

The electrochemical performance of the Pd/Gr/GCE sensor was quantitatively analyzed by SWV under optimal conditions for aggregation using different concentrations of OMT and DCV individually. By means of the SWV optimised conditions, as previously described, the proposed Pd/Gr/GCE was applied to investigate the electrochemical response as a function of the OMT and DCV concentrations. All measurements were made in triplicate.

The analytical response shown in Fig. 7, has a linear response in the range of 3.5×10^{-8} M to 1.25×10^{-5} M for both OMT and DCV. The results of these experiments individually are shown in Fig.8A & B. When the concentration of OMT and DCV were increased from 3.5×10^{-8} M to 1.25×10^{-5} M, the reduction peak current increased linearly. The linear regression equation for this region was: $Y = -60.857x + 4.667$, $Y = -64.571x + 1$ with correlation coefficients of $R^2 = 0.9975$, 0.9939 and a limit of detections ($S/N = 3$) are 2.47×10^{-10} M and 3.28×10^{-10} M for OMT and DCV respectively. Thus, Pd/Gr/GCE has good electrocatalytic activity and adsorption capacity towards high concentrations OMT and DCV.

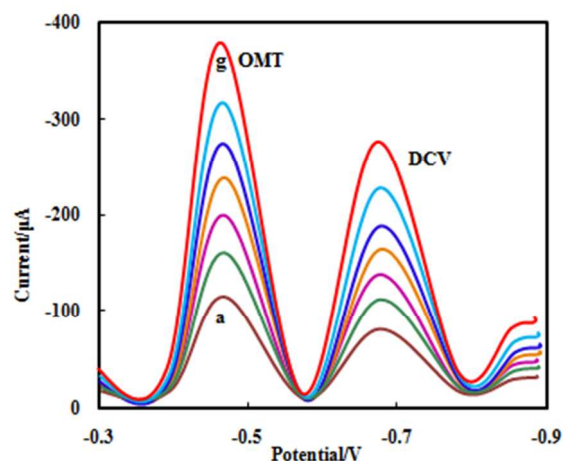


Fig. 7 Simultaneous SWV responses of OMT and DCV at Pd/Gr/GCE in PB solution (pH 5.0) with increasing concentrations (a-g) 3.5×10^{-8} M to 1.25×10^{-5} M.

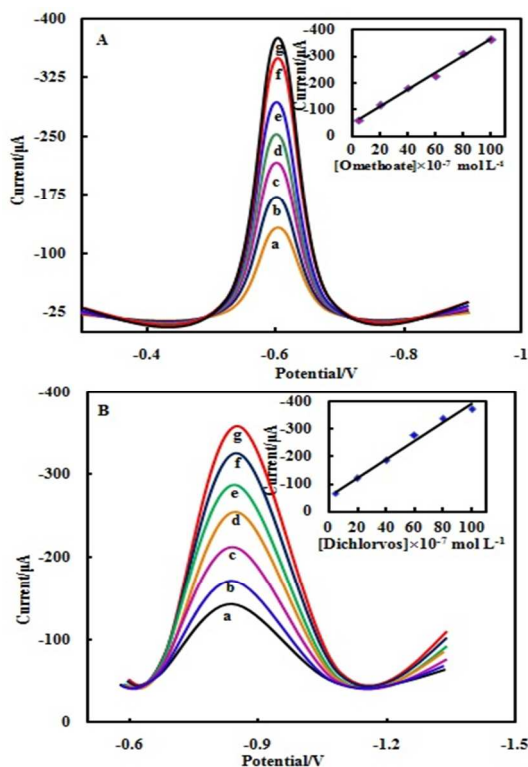


Fig.8 SWV responses of OMT (A) and DCV (B) at Pd/Gr/GCE in PB solution (pH 5.0) with increasing concentrations (a-g) 3.5×10^{-8} M to 1.25×10^{-5} M.

3.7. Pre-treatment of real samples

A fresh grain samples (mean weight 5gm) was pulverised by a blender and was placed in a 250 ml volumetric flask. Because the concentration of pesticides in grain samples is too low for direct detection, 2.0 ml of each of the standard solutions of the pesticides were sampled by pipetting. This aliquot was transferred to a flask containing 50.0 ml ethanol and 50gm anhydrous sodium sulphate was added to remove any water. Addition of 0.5gm activated charcoal then facilitated the removal of interfering colouring matter. The mixture was shaken for 30 min and accordingly the organophosphorous pesticides in the grain samples were extracted into the methanol phase. The sample was filtered, 25.0 ml of the methanol solution was transferred into an evaporating dish and reduced by flowing nitrogen gas in a cell to 5 ml. This aliquot was diluted to 10 ml with distilled water.

3.8. Determination of the pesticide in grain samples

The familiar grains, green peas and field bean were chosen for analysis. Each sample of the grains was treated as described in the above and then 0.1 ml of the extract was transferred to the electrochemical cell for analysis. The calibration was selected for the analysis of the grain extracts. The results (Table 1) showed that values of the pesticides found in the grain samples were in the range of $3.5 \times 10^{-8} \text{M}$ to $1.25 \times 10^{-5} \text{M}$ and the procedure was further validated by standard addition of the given pesticides. This showed good recovery values in the range of 96.00% – 99.71%.

Table 1. Recovery study of OMT and DCV in grain samples

Samples	Added(M)	Found(M)	*Recovery (%)	RSD
Green Peas	1.25×10^{-5}	1.23×10^{-5}	98.40	1.75
	2.25×10^{-6}	2.23×10^{-6}	99.11	2.05
	3.50×10^{-7}	3.48×10^{-7}	99.42	2.15
	3.50×10^{-8}	3.49×10^{-8}	99.71	2.24
Field Bean	1.25×10^{-5}	1.20×10^{-5}	96.00	0.78
	2.25×10^{-6}	2.21×10^{-6}	98.22	1.63
	3.50×10^{-7}	3.47×10^{-7}	99.14	2.10
	3.50×10^{-8}	3.48×10^{-8}	99.42	2.15

*Average of five determinations

3.9. Calibration curves and limits of detection

The individual pesticides were carried out according to the sample procedure. Calibration plots based on the dependence of the peak current on concentration were linear, and in addition to the parameters of the calibration models, the precision of determination for these compounds was also established by analysing five known solutions containing the lowest concentration on the calibration graph. The relative standard deviation (R.S.D) values obtained from 0.78 to 2.24 % for OMT and DCV respectively. The detection limit values were found to be $2.47 \times 10^{-10} \text{M}$ and $3.28 \times 10^{-10} \text{M}$ for OMT and DCV respectively, which compare well with the detection limits, obtained previously.³⁶⁻³⁸ Thus, these results clearly indicate that the proposed electrochemical method of analysis is reliable for the determination of individual pesticides (Fig.8). However, it should be noted that the linear calibration relationships were observed only at the actual peak potential. These changes showed small progressive peak potential shifts to more negative values with increase in concentration.

3.1.1. Reproducibility and stability

The stability of the Pd/Gr/GCE was investigated by CV (Figure not shown). The Pd/Gr/GCE exhibits good measurement stability by consecutive 10 cycles of CV test, a little decrease of peak current was observed with increase of scanning cycle, but the reduction peak current retained 99 % of its initial current after it was tested by consecutive CV scan. This indicates that the Pd/Gr/GCE film did not unwrap from the surface of GCE through 10 times of CV cycles. The long term stability of the electrode was investigated by the CV measurement, after storage in the air, for one week at room temperature and the result shows that about 4% of its initial current was loss. The elevated stability of the film can be owing to the GCE was used as substrate which can improve the interaction force between GCE and high conductive particles of Pd, so the film can be strongly coated on the GCE; another reason is that graphene has good stability properties for immobilization of Pd.

3.1.2. Interferences

The coexisting substances were occupied into account for applications. In the study, $5 \mu\text{g}$ of OMT and DCV was selected as a typical concentration. The liberal maximum concentration of the coexisting substance was determined, in which the substance caused Pd/Gr/GCE intensity change of approximately ± 3 . We also study the effect of the inorganic ions like NH_4^+ , Ca^{2+} , Zn^{2+} , Fe^{3+} , SO_4^{2-} , Cl^- , CO_3^{2-} and PO_4^{3-} and found that they did not affect the results and some other organophosphorous pesticides, such as parathion-methyl, trichlorfon and dichlorvos, do not interfere. The interferences of some metal ions, such as Pb^{2+} , Hg^{2+} , Cu^{2+} and Ag^+ can be removed by the alkaline hydrolysis procedure.²⁶ In our study, other organophosphorous pesticides in this optimized condition are hardly to be detected, so the method to determination of OMT and DCV is very perceptive.

4. Conclusions

A newly modified composite electrode was developed using palladium (Pd) and graphene (Gr) nanocomposite, which can be used for the simultaneous determination of OMT and DCV in grain samples. The Pd/Gr/GCE nanocomposite was successfully characterised by SEM and CV, which indicated that the Pd nanoparticles were supported on the Gr/GCE surface. Furthermore, the synergistic effect of the Gr and Pd nanoparticle yielded lower LODs and improved the reproducibility, repeatability and the sensitivity of the composite electrode for the simultaneous determination of OMT and DCV. Additionally, the electrode showed long-term stability. Finally, the Pd/Gr/GCE composite electrode can be an effective material for simultaneous electrochemical determination of OMT and DCV and also is an alternative material to be used in environmental analysis.

Acknowledgement

This work was supported by the DAE-BRNS, Mumbai, India (No: 2013/37C/22/BRNS) was gratefully acknowledged.

Affiliation

Sri Venkateswara University - Electroanalytical Lab, Department of Chemistry, Tirupati, Andhra Pradesh, India

References

1. S. Y. Wang, D. S. Yu, L. M. Dai, D.W. Chang, J.-B. Baek, *ACS Nano*, 2011, 5, 6202.

2. C. N. R. Rao, A. K. Sood, K. S. Subrahmanyam, A. Govindaraj, *Angew. Chem. Int. Ed.*, 2009, 48, 7752.
3. K. S. Novoselov, A. K. Geim, S. V. Morozov, D. Jiang, M. I. Katsnelson, I. V. Grigorieva, S. V. Dubonos, A. A. Firsov, *Nature*, 2005, 438, 197.
4. B. Wang, J. Park, Ch. Y. Wang, H. Ahn, G. X. Wang, *Electrochim. Acta*, 2010, 55, 6812.
5. Z. Liu, B. Zhao, C. Guo, Y. Sun, Y. Shi, H. Yang, Z. Li, *J. Colloid Interface Sci.*, 2010, 351, 233.
6. Y.-H. Qin, H. H. Yang, X.-S. Zhang, P. Li, X.-G. Zhou, L. Niu, W. K. Yuan, *Carbon*, 2010, 48, 3323.
7. Y. Wang, Z. Min, H. Yang, S. Ping, C. Ming, *Int. J. Hydrogen Energy*, 2010, 35, 10087.
8. S. Park, J. An, I. Jung, R.D. Piner, S. J. An, X. Li, A. Velamakanni, R.S. Ruoff, *NanoLett.*, 2009, 9, 1593–1597.
9. Y. Li, X. Fan, J. Qi, J. Ji, S. Wang, G. Zhang, F. Zhang, *NanoRes*, 2010, 3, 429–437.
10. J. Liu, W. Zhou, T. You, F. Li, E. Wang, S. Dong, *Anal. Chem.*, 2010, 68, 3350–3353.
11. Z. Liu, B. Zhao, C. Guo, Y. Sun, Y. Shi, H. Yang, Z. Li, *J. Colloid Interface Sci.*, 2010, 351, 233–238.
12. A.F. Littke, G.C. Fu, *Angew. Chem. Int. Ed.*, 2002, 41, 4176–4211.
13. B. Lim, M. Jiang, J. Tao, P.H.C. Camargo, Y. Zhu, Y. Xia, *Adv. Funct. Mater.*, 2009, 19, 189–200.
14. M.T. Reetz, E. Westermann, *Angew. Chem. Int. Ed.*, 2000, 9, 165–168.
15. M.R. Kim, S.H. Choi, *J. Nanomater.*, 2009, 15.
16. Y. Nishihata, J. Mizuki, H. Tanaka, M. Uenishi, M. Kimura, *J. Phys. Chem. Solids*, 2005, 66, 274–282.
17. Y. Xiong, J.M. Mc Lellan, J. Chen, Y. Yin, Z. Y. Li, Y. Xia, *J. Am. Chem. Soc.*, 2005, 127, 17118–17127.
18. L. Meng, J. Jin, G. Yang, T. Lu, H. Zhang, C. Cai, *Anal. Chem.*, 2009, 81, 7271–7280.
19. Muniyandi Rajkumar, Balamurugan Devadas, Shen-Ming Chen, Pin-Chun Yeh, *Colloids and surfaces A: Physicochem. Eng. Aspects*, 2014, 452, 39–45.
20. Qiyu Wang, Xiaoqiang Cui, Weiming Guan, Weitao Zheng, Jianli Chen, Xianliang Zheng, Xiaoming Zhang, Chang Liu, Tianyu Xue, Haitao Wang, Zhao Jin, Hong Teng, *Journal of Physics and Chemistry of Solids*, 2013, 74, 1470–1474.
21. Selvakumar Palanisamy & Shuhao Ku & Shen-Ming Chen, *Microchim Acta*, 2013, 180:1037–1042
22. Hongfang Liu, Xianlan Chen, Linhong Huang, Jian Wang and Haibo Pan, *Electroanalysis*, 2014, 26, 556 – 564
23. Guohui Chang, Yonglan Luo, Wenbo Lu, Xiaoyun Qin, Abdullah Mohamed Asiri, Abdulrahman Obaid Al-Youbi and Xuping Sun, *American Journal of Nanotechnology*, 2013, 4 (1): 1-7.
24. Jian-Jun Shi, Jun-Jie Zhu, *Electrochimica Acta*, 2011, 56, 6008–6013.
25. Zhixiang Zheng, Yongling Du, Qingliang Feng, Zaihua Wang, Chunming Wang, *Journal of Molecular Catalysis A: Chemical*, 2012, 353–354, 80–86.
26. Wang Yu, Sun Yuansi, Huang Junhua, Zhang Wuming, Zhou Xingyao, *Wuhan University Journal of Natural Sciences*, 1998, 3, 4, 469-472.
27. Roach J A G, Carson L J. *J. Asso Off Anal Chem*, 1987, 70, 3 : 439-442
28. Ferreira J R, Faleao M M, Tainha A. *J Agric Food Chem*, 1987, 35, 4: 506-508.
29. Drescher W, Fiedler L. Methode zum Nachweis von Ruckstanden der, *Chemosphere*, 1983, 12: 1605-1610
30. Y. Wang, Y. Sun, J. Huang et. al., *Wuhan University J. Nat. Sci.*, in press.
31. J. Ngeh-Ngwainbi, A.A. Suleiman, G.G. Guil, *Bault, Biosens. Bioelectron.* 1990, 5, 13.
32. L.V. Rajakovic, S. Strbac, *Anal. Chim. Acta*, 1995, 315, 83.
33. Y. Tomita, G.G. Guilbault, *Anal. Chem.*, 1980, 52, 1484.
34. G.G. Guilbault, J. Affolter, Y. Tomita, *Anal. Chem.*, 1981, 53, 2057.
35. Fang Cheng, Wang Xianbao, Zhang Wuming, *Talanta*, 1999, 49, 253–259
36. Djenaine De Souza, Sergio A. S. Machado, *Anal Bioanal Chem*, 2005, 382: 1720–1725.
37. Yanhong bai, Jierong chen, Huimu, Chunhong zhang and Baoping li, *j. agric. food chem.* 2009, 57, 6238–6245.
38. Yugui Tao, Yaoming Wang, Lianbin Ye, Hefei Li, Qiang Wang, *Bull Environ Contam Toxicol*, 2008, 81:210–215.
39. Sivaprasad M, Swarupa Ch, Dhananjayulu M, Jayapal MR and Sreedhar NY, *J Anal Bioanal Tech*, 2014, 5:192 doi:10.4172/2155-9872.1000192.
40. L. Han, X. Zhang, *Electroanalysis*, 2009, 21, 124.